THE JOURNAL OF BIOLOGICAL CHEMISTRY
Vol. 276, No. 25, Issue of June 22, pp. 22991–22999, 2001

Printed in U.S.A.

A Conserved Asn in Transmembrane Helix 7 Is an On/Off Switch in the Activation of the Thyrotropin Receptor*

Received for publication, March 13, 2001, and in revised form, April 12, 2001
Published, JBC Papers in Press, April 18, 2001, DOI 10.1074/jbc.M102244200

Cédric Govaerts‡§¶, Anne Lefort‡, Sabine Costagliola‡, Shoshana J. Wodak§, Juan A. Ballesteros‖, Jacqueline Van Sande‡, Leonardo Pardo, and Gilbert Vassart‡ ‡‡**

*From the ‡Institut de Recherche Interdisciplinaire en Biologie Humaine et Nucléaire, Université Libre de Bruxelles, Campus Erasme, 808 route de Lennik, B-1070 Bruxelles, Belgium, the **Laboratori de Medicina Computacional, Unitat de Bioestadística, Facultat de Medicina, Universitat Autònoma de Barcelona, 08193 Bellaterra, Spain, the §Service de Conformation des Macromolécules Biologiques, Université Libre de Bruxelles, CP 160/16, Avenue F. Roosevelt, 1050 Bruxelles, Belgium, and the ‖Novasite Pharmaceuticals, Inc., San Diego, California 92121*

The thyrotropin (TSH) receptor is an interesting model to study G protein-coupled receptor activation as many point mutations can significantly increase its basal activity. Here, we identified a molecular interaction between Asp^{633} in transmembrane helix 6 (TM6) and Asn^{674} in TM7 of the TSHr that is crucial to maintain the inactive state through conformational constraint of the Asn. We show that these residues are perfectly conserved in the glycohormone receptor family, except in one case, where they are exchanged, suggesting a direct interaction. Molecular modeling of the TSHr, based on the high resolution structure of rhodopsin, strongly favors this hypothesis. Our approach combining site-directed mutagenesis with molecular modeling shows that mutations disrupting this interaction, like the D633A mutation in TM6, lead to high constitutive activation. The strongly activating N674D (TM7) mutation, which in our modeling breaks the TM6-TM7 link, is reverted to wild type-like behavior by an additional D633N mutation (TM6), which would restore this link. Moreover, we show that the Asn of TM7 (conserved in most G protein-coupled receptors) is mandatory for ligand-induced cAMP accumulation, suggesting an active role of this residue in activation. In the TSHr, the conformation of this Asn residue of TM7 would be constrained, in the inactive state, by its Asp partner in TM6.

The TSH,[1] LH/CG and FSH receptors constitute a subfamily of G protein-coupled receptors (GPCR) characterized by large amino-terminal ectodomains responsible for high affinity binding of their natural agonists, the glycoprotein hormones (1, 2). These ectodomains are made essentially of leucine-rich repeats, a protein fold frequently found to be involved in protein-protein interactions (3–5). The serpentine portion of these receptors, responsible for signal transduction, comprises seven transmembrane helices, showing significant similarity with the transmembrane portions of rhodopsin-like GPCRs; they are therefore grouped with them into family 1 of GPCRs.

The glycohormone receptors thus present a clear dichotomy between the agonist-binding and signal-transduction domains, with the mechanism of interaction between the two domains, responsible for receptor function, remaining largely unknown. Sequences displaying strong similarities with the glycohormone receptors have been identified in *Anthopleura elegantissima, Drosophila,* and *Caenorhabditis elegans* (6–9). Related receptors have also been discovered in mammals (10, 11). But for all of these cases, the nature of the agonists remains to be identified.

Several characteristics make the TSH receptor an interesting system to study the mechanisms of receptor activation: (i) the wild type receptor has been shown to display significant basal activity (12–14); (ii) mutations involving more than 20 different residues have been shown to increase its constitutive activity, causing autonomous thyroid adenomas or non-autoimmune hereditary hyperthyroidism (15); (iii) loss of function mutations have also been described, abolishing basal activity (16) or affecting agonist-induced response (17, 18).

Interestingly, naturally occurring activating mutations are more rarely found in the LH/CGr (19), and almost never found the FSHr (20). Indeed, no spontaneous activating mutation has been identified in the FSH receptor except for a single case with an unusual phenotype (21). These data reflect a difference in the structural constraints keeping the various glycoprotein hormone receptors in the inactive state. The wild type TSH receptor displaying constitutive activity and being easily activated by mutations would be the less constrained, followed by the LH receptor, devoid of constitutive activity but susceptible to activation by mutations. The FSH receptor would be the most constrained, as it is silent in the absence of stimulation by agonist and difficult to activate by mutations.

The high resolution crystal structure of bovine rhodopsin determined recently (22) provides for the first time a detailed atomic description of a GPCR molecule in an inactive conformation, and represents a solid basis for modeling the structures of other rhodopsin-like GPCRs. Such models can then be used to help rationalize the many observations made on the relations between conserved sequence feature and functional properties. Conservation of functionally important sequence motifs within this receptor family has been interpreted as meaning that the basic characteristics of the rhodopsin fold, as

* This work was supported in part by the Belgian State, Prime Minister's office, Service for Sciences, Technology, and Culture, grants from the Fonds de la Recherche Scientifique Médicale, Fonds National de la Recherche Scientific, Association Recherche Biomédicale et Diagnostic, and BRAHMS Diagnostics, Comision Interministerial de Ciencia y Tecnologia Grant SAF99-073, Fundació La Marató TV3 Grant 0014/97, Improving Human Potential of the European Community Grant HPRI-CT-1999-00071.

¶ Fellow of the Fonds pour la Formation à la Recherche dans l'Industrie et dans l'Agriculture.

‡‡ To whom correspondence should be addressed: IRIBHN, Université Libre de Bruxelles, Campus Erasme, 808 route de Lennik, B-1070 Bruxelles, Belgium. Tel.: 32-2-555-41-71; Fax: 32-2-555-46-55; E-mail: gvassart@ulb.ac.be.

[1] The abbreviations used are: TSH, thyroid-stimulating hormone; GPCR, G protein-coupled receptor; TM, transmembrane helix; LH, lutenizing hormone; CG, chorionic gondadotropin; FSH, follicle stimulating hormone; wt, wild type; PCR, polymerase chain reaction.

well as the molecular mechanisms leading to receptor activation are similar in the different receptor subtypes. Among such conserved sequence motifs are prolines in transmembrane helices (TM) 6 and 7 and charged residues in TM2 and TM3 (the Asp and Arg of the canonical "DRY" motif). However, considering the extreme diversity of the natural agonists of the different receptors it has also been accepted that different receptor subtypes may have evolved quite specific structural and functional features, probably reflected in the specific sequence signatures of each subtype.

Multiple alignments of the glycohormone receptor sequences reveal one such signature: a conserved Asp residue in TM6 at position *6.44*^{633} (corresponding to residue 633 in the TSHr sequence; see "Experimental Procedures"). Most other GPCRs harbor a Phe or a Tyr at this position. Natural mutations of residue *6.44*^{633} in the TSHr and LH/CGr were shown to lead to constitutive activation, causing autonomous toxic thyroid adenomas (12) and male limited pseudoprecocious puberty (23), respectively. This suggested that D*6.44*^{633} might play a role in the mechanism of receptor activation. Recent *ex vivo* transfection studies suggested that this residue is important for maintaining the inactive conformation of the LH receptor (24), in agreement with earlier molecular modeling studies, according to which the inactive form of the LH receptor would require the formation of H-bonds between TM6 and TM7, involving residues Thr*6.43*, Asp*6.44*, Asn*7.45,* and Asn*7.49* (25).

In the present study, we analyzed the multiple alignments of 44 glycohormone and closely related receptors. This lead to the observation that residues D*6.44* and N*7.49* (the Asn of the conserved NP*XX*Y motif in TM7) are both conserved in glycohormone receptors, except in one of two *Drosophila* receptors (6), where they are exchanged (this receptor bearing N*6.44* and D*7.49*). Since such coordinated mutations may reflect spatial interactions between the residues (26, 27), our observation was interpreted as indicating the existence of an interaction between D*6.44* and N*7.49*. Considering the activating effect of amino acid substitutions at position *6.44*, we formulate the hypothesis that this interaction is required in order to maintain the TSH receptor in an inactive conformation. We then investigated this hypothesis by combining computational and experimental approaches.

Molecular modeling techniques were used to derive the atomic coordinates of the transmembrane region of the TSHr, using as template the corresponding region of the high resolution structure of rhodopsin. To analyze the conformational properties of residues *6.44* and *7.49* and their surroundings in the resulting model, molecular dynamics simulations were carried out in the presence of explicit methane molecules, mimicking the non-polar environment of the membrane. This was done for both the wt receptor and for several substitution mutants of residues that are likely to affect the proposed interaction. In parallel, the same mutants were engineered into human TSHr using site-directed mutagenesis and their effects on receptor expression, hormone binding, and activation were measured.

The results provide compelling evidence that D*6.44* and N*7.49* do interact in the inactive TSHr and that disruption of this interaction, by mutating either the *6.44* or the *7.49* residues, results in constitutive activation. Furthermore, combining our observations with data from other GPCRs is shown to yield new insights into the general mechanism of GPCR activation

EXPERIMENTAL PROCEDURES

Numbering Scheme of GPCRs—The standardized numbering system of Ballesteros and Weinstein (28) was used throughout to identify residues in the transmembrane segments of different receptors. Each residue is identified by two numbers: the first (1 through 7) corresponds to the helix in which it is located; the second indicates its position relative to the most conserved residue in that helix, arbitrarily assigned to 50. For instance, N*7.49* is the asparagine in transmembrane helix 7 (TM7), located 1 residue before the highly conserved proline P*7.50*. Residue D*2.50* corresponds to Asp^{460} in the TSHr numbering; S*3.36* to Ser^{505}; S*3.39* to Ser^{508}; T*6.43* to Thr^{632}; D*6.44* to Asp^{633}; N*7.45* to Asn^{670}, and N*7.49* to Asn^{674}.

Molecular Modeling and Molecular Dynamics Simulation of the Transmembrane Bundle—The atomic model of the transmembrane domain of the TSHr was built by comparative modeling techniques, using as template the atomic coordinates of the transmembrane domain of bovine rhodopsin (22). The sequences of the 2 proteins in this region were aligned so as to equivalence the positions of the following conserved residues: Asn^{55}-Asn*1.50*^{432} (the superscripts represent the residue numbering in rhodopsin structure PDB code 1F88, and human TSHr sequence, respectively, and *1.50 is* the numbering in the standardized nomenclature), Asp^{83}-Asp*2.50*^{460}, Arg^{135}-Arg*3.50*^{519}, Trp^{161}-Trp*4.50*^{546}, Pro^{215}-N*5.50*^{590}, Pro^{267}-Pro*6.50*^{639}, and Pro^{303}-Pro*7.50*^{675}. The conformations of these side chains were kept as in the rhodopsin crystal structure. Those of the non-conserved amino acids were built using a rotamer library specific for α-helices. (29). Ionizable groups in the helices were modeled as uncharged except for Asp*2.50*, Glu*3.37*, Glu*3.49*, Arg*3.50*, Asp*6.30*, and Asp*6.44*.

To relieve residual strain resulting from suboptimal positioning of the side chains, the resulting model was first subjected to energy minimization (1000 steps), and then to a simulated annealing procedure, using molecular dynamics. This involved heating to 600 K for 30 ps (1 ps = 10^{-12} s), equilibration for 120 ps at 600 K, cooling to 300 K for 60 ps, and equilibration for 90 ps at 300 K. During this processes the C_α atoms and the side chains of conserved residues were kept fixed at their positions in the rhodopsin crystal structure.

Molecular models for the mutant receptors containing the single substitutions D*6.44*N, D*6.44*A, N*7.49*D, and N*7.49*A and double substitution D*6.44*N-N*7.45*D and D*6.44*N-N*7.49*D, were built using, as the starting point the final model derived for the wt TSHr and optimizing the conformations of the substituted side chains using an analogous procedure to that described above. This procedure was deemed reasonable, since the considered substitutions were either isosteric, replacement of Asn by Asp, or vice versa, or side chain deletion (replacement by Ala).

To investigate the structural properties of the modeled conformations, room temperature molecular dynamics simulations were used. In order to mimic the hydrophobic environment of the membrane, these simulations were carried out in the presence of explicit methane molecules, and using periodic boundary conditions. The periodic box was ~73 Å × 63 Å × 52 Å in size, and contained between 4219 and 4241 methane molecules in addition to the transmembrane domain. Similar conditions have been recently used to mimic the membrane environment in molecular dynamics simulations of the potassium channel (30).

To start the simulation protein portion was kept fixed while the methane molecules were energy minimized (500 steps), then heated to 300 K for 15 ps and equilibrated for another 35 ps. Following this, the same procedure was repeated on the entire protein-solvent system but with an equilibration run of 250 ps; a 250 ps production trajectory was then generated at constant volume using the Particle Mesh Ewald method for computing electrostatic interactions (31). For analysis purposes, structures were collected every 2 ps. The simulations were performed with the Sander module of AMBER 5 (32), the all-atom force field (33), SHAKE bond constraints on all bonds, a 2 fs integration time step, and constant temperature of 300 K coupled to a heat bath.

Site-directed Mutagenesis of the TSH Receptor—Plasmids encoding the various TSHr mutants were constructed by site-directed mutagenesis using two subsequent PCR amplifications rounds. This procedure requires two partially overlapping complementary primers containing the mutation and two external primers. Two distinct PCRs are performed on TSHr template by using in one tube the direct mutagenic primer and the external reverse primer and in the other tube the reverse mutagenic primer and the external direct primer. One μl of each PCR product was mixed and used as template in a subsequent PCR amplification with the two external primers. The resulting amplified fragment contains the mutation and can be cloned after digestion with *Bsu*36I and *Bam*HI into the pSVL expression vector (Amersham Pharmarcia Biotech, Freiburg, Germany) containing the wild type TSHr (34) using standard procedures. All PCR-generated receptor fragments were verified by sequencing before transfection.

Transfection and Assays—COS-7 cells were grown in Dulbecco's modified Eagle's medium supplemented with fetal bovine serum (10%),

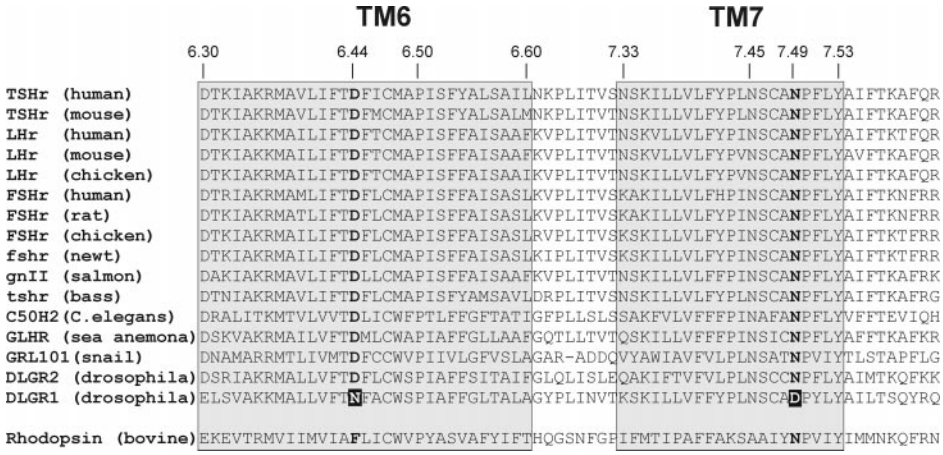

FIG. 1. **Multiple sequence alignment of TM6-ECL3-TM7 of glycohormone receptors and bovine rhodopsin.** For the sake of clarity, representative sets of sequences from mammals and bird glycohormone receptors are shown together with related sequences from fish, insects, sea anemone, and *C. elegans*. The generalized numbering scheme (see "Experimental Procedures") is used to label the alignment. Residues *6.44* and *7.49* are in *bold* characters, the residue exchange is *highlighted*. The corresponding sequence of bovine rhodopsin is also aligned. The limits of the helices have been defined according to those observed in the rhodopsin structure (22). Accession numbers for the non-mammalian sequences are: Q90674 (LHr chicken), P79763 (FSHr chicken), AB005587 (fshr newt), AB030005 (gnII salmon), AF239761 (tshr bass), T20123 (C50H2 *C. elegans*), P35409 (GLHR sea anemona), P46023 (GRL101 snail), AF142343 (LGR2 *Drosophila*), and U47005 (LGR1 *Drosophila*).

sodium pyruvate (1 mM), penicillin (100 IU/ml), streptomycin (100 μg/ml), and fungizone (2.5 μg/ml). Cells were seeded at a density of 150,000 or 300,000 cells/3-cm dish. One day later, they were transfected (250 or 500 ng of DNA/dish, respectively) by the DEAE-dextran method followed by a dimethyl sulfoxide shock (35). Two days after transfection, cells were used for flow immunocytofluorometry, cAMP and ^{125}I-TSH binding studies. Duplicate dishes were used for each assay. Each experiment was repeated at least three times. Cells transfected with pSVL alone were always run as controls.

Flow Immunocytofluorometry—Cells were detached from the plates with phosphate-buffered saline containing EDTA and EGTA (5 mM each) and transferred into Falcon tubes (2052). Cells were centrifuged at 500 $\times$ *g*, at 4 °C for 3 min and the supernatant was removed by inversion. They were incubated for 30 min at room temperature with 100 μl of phosphate-buffered saline/bovine serum albumin (0.1%) containing the BA8 monoclonal antibody, obtained from genetic immunization with the wild type TSH receptor cDNA (36). The cells were washed with 4 ml of phosphate-buffered saline/bovine serum albumin (0.1%) and centrifuged as above. They were incubated for 30 min on ice in the dark with fluoresceine-conjugated γ-chain-specific goat anti-mouse IgG (Sigma) in the same buffer. Propidium iodide (10 μg/ml) was used for detection of damaged cells which were excluded from the analysis. Cells were washed once again and resuspended in 250 μl of phosphate-buffered saline/bovine serum albumin (0.1%). The fluorescence of 10,000 cells per tube was assayed by a FACScan Flow Cytofluorometer (Beckton Dickinson, Erembodegem, Belgium).

cAMP Determination—Cells were washed with Krebs-Ringer-Hepes buffer (KRH isotonic, pH 7.4). After a preincubation in KRH at 37 °C for 30 min, cells were incubated in the same buffer supplemented with Rolipram 25 μM (a cAMP phosphodiesterase inhibitor, gift from the laboratory of J. Logeais, Paris, France), in the absence or presence of various bTSH concentrations (Sigma). One hour later, the medium was removed and 0.1 M HCl was added to the cells. The cellular extracts were dried overnight in a vacuum concentrator (Savant) and intracellular cAMP was determined exactly as described previously (37). Basal cAMP was normalized to cell surface expression for each of the constructs. To this end, specific cAMP accumulation (= cAMP of receptor-transfected cells − cAMP of the pSVL-transfected cells) is divided by the specific FACS value (= fluorescence of receptor-transfected cells − fluorescence of pSVL-transfected cells), which can be summarized as: specific basal activity = (cAMP(receptor) −cAMP(pSVL))/(FACS-(receptor) − FACS (pSVL)). The values are then expressed as percentage of specific basal activity of the wt TSHr.

Binding Assays—Two days after transfection, cells were washed twice with NaCl-free Hank's buffer supplemented with 280 mM sucrose. Cells were incubated at room temperature in this medium (supplemented with low fat milk, 2.5%) containing about 100,000 counts/ml ^{125}I-TSH (TRAK Assays, BRAHMS Diagnostica, Berlin; 58 μCi/μg, 50–60 units/mg) and various concentrations of unlabeled TSH (Sigma). Four hours later, the cells were rinsed twice with chilled Hank's buffer and solubilized by 1 N NaOH. Bound radioactivity was determined in a γ-scintillation counter. Under our conditions, the radioactivity nonspecifically bound to COS cells expressing the TSH receptor (defined as the radioactivity bound to the dish in the presence of 100 milliunits/ml unlabeled TSH) was identical to that bound to mock-transfected cells. In the absence of a consensus about the bioactivity of pure bovine TSH, we have expressed all TSH or TSH receptor concentrations in milliunits/ml, assuming a 1:1 stoichiometry for TSH binding to its receptor. The competition binding curves have been fitted by nonlinear regression, assuming a single receptor site, using the Prism3 program (GraphPad Softwares).

RESULTS

Sequence Alignment of the Glycohormone Receptor Subfamily

Multiple sequence alignment of the sixth and seventh transmembrane helices of 44 glycohormone and closely related receptors was performed. Fig. 1 shows the alignment of representative sequences, together with that of bovine rhodopsin. Inspection of this alignment reveals two key sequence motifs characteristic of the rhodopsin-like family: the P*6.50* in TM6 and the NP*XX*Y motif in TM7. A noteworthy difference is the presence of Asp at position *6.44* instead of the more common Phe or Tyr, which represent more than 81% of the rhodopsin-like receptors found in the GPCRDB (38). D*6.44* is completely conserved throughout the glycohormone family of GPCR, from *C. elegans* to human, with only a single exception, the *Drosophila* DLGR1 sequence (accession number U47005 (6)), which contains an Asn residue. Interestingly, this change is correlated with the replacement of the highly conserved Asn at position *7.49* by Asp. Swapped mutations of this kind suggest interaction between the corresponding residues in the three-dimensional structures (26, 27). We could indeed verify that in the rhodopsin structure, the C_α of Phe*6.44* and Asn*7.49* (the conserved N of the NP*XX*Y motif) were facing each other at a distance of 11 Å, sufficient to allow direct interaction between the side chains. Given that a series of amino acid substitutions at D*6.44* found in thyroid adenomas result in a significant increase in the constitutive activity of the TSHr, we then made the hypothesis that interactions between the D*6.44* and N*7.49* side chains are important in maintaining the receptor in its inactive conformation.

Molecular Dynamics Simulation of the Transmembrane Region of the TSHr

In order to investigate the proposed interaction between D*6.44* and N*7.49* in the context of the entire helix bundle, the

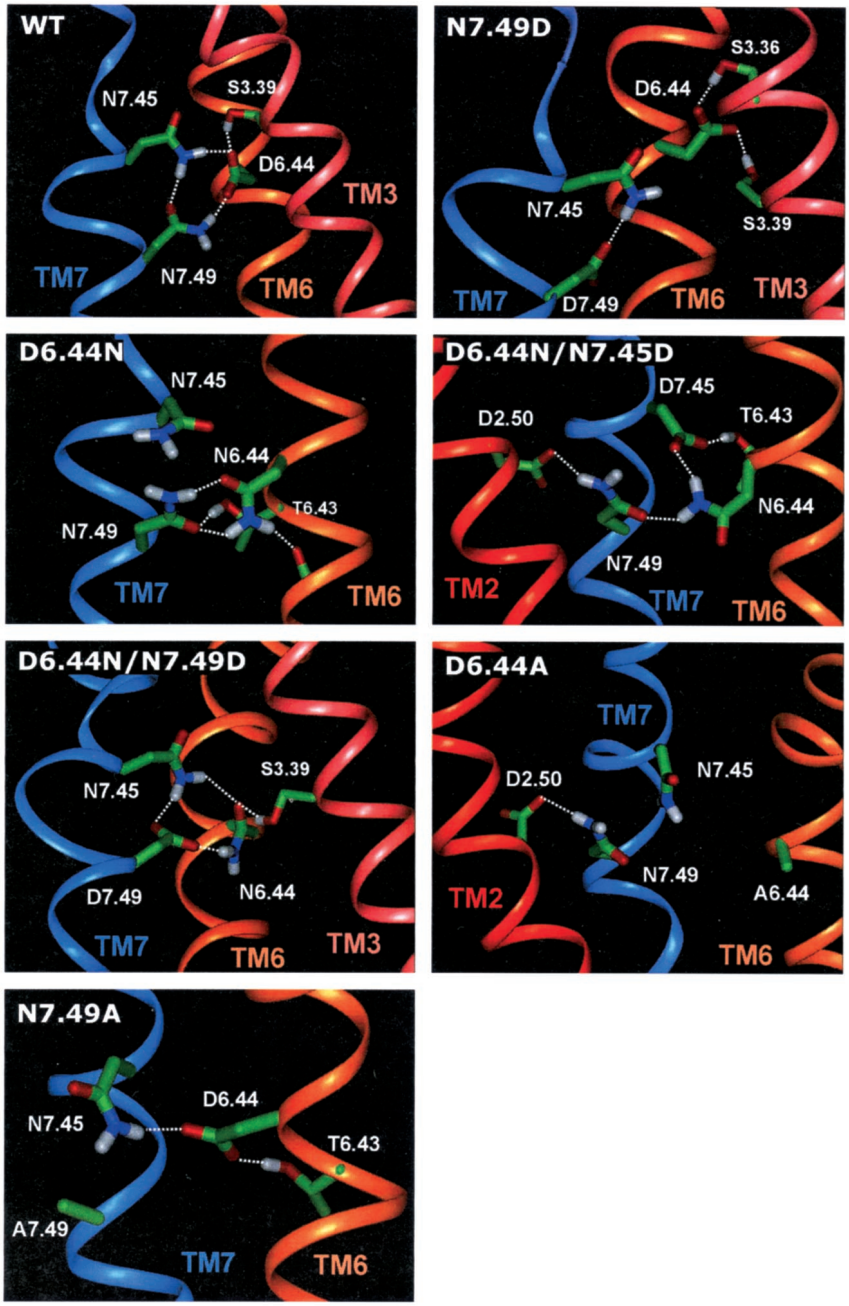

FIG. 2. **Representative structures of the different models.** For each of the seven models, a representative structure was selected from the set collected during the production phase of the Molecular Dynamics simulation. Each panel is labeled according to the name of the mutant represented. A local view on the TM6-TM7 locus is shown, with the TM helices represented as *ribbons*. Side chains are shown as *solid sticks* for the residues implicated in the motif of interest. Carbon atoms are in *green*, nitrogen in *blue*, oxygen in *red,* and hydrogen in *white*. Hydrogen bonds are sketched as *dotted white lines*. The generalized numbering scheme (see "Experimental Procedures") is used to label the different residues.

molecular model of the transmembrane domain of the TSHr was built, based on the high-resolution structure of bovine rhodopsin. This model was then subjected to unrestrained molecular dynamics simulations in the presence of explicit methane molecules mimicking the apolar membrane environment (see "Experimental Procedures"). Having ascertained that the helical segments conserved their secondary structure and that the bundle remained well packed and maintained the rhodopsin fold throughout the trajectory, we analyzed the polar interactions made between TM6 and TM7. In particular, we computed the average hydrogen-acceptor distances in conformations along the trajectory, and the fraction of the conformations in which the bond was formed.

All throughout the simulation D*6.44* and N7*.49* were seen to form a hydrogen bond between the D*6.44* $O_{\delta 1}$ and N7*.49* $N_{\delta 2}H$ atoms, with an average O-H distance of 1.9 Å (see Fig. 2 for a representative structure). The TM6-TM7 interaction involved in addition a more complex hydrogen bond network. N7*.45*, located one helix turn prior to N7*.49*, formed 2 H-bonds. One, with D*6.44* ($N_{\delta 2}{}^{7.45}H\text{-}O_{\delta 2}{}^{6.44}$; average distance 2.0 Å) and another with N7*.49* ($N_{\delta 2}{}^{7.45}H\text{-}O_{\delta 1}{}^{7.49}$; average distance of 1.9 Å). The hydrogen bond between D*6.44* and N7*.45*, thus provides a second polar interaction between TM6 and TM7. In addition, the D*6.44* $O_{\delta 2}$ was seen to form and H-bond with $O_{\gamma}H$ group of the conserved S*3.39*, in TM3 (average distance of 1.8 Å), establishing a polar interaction between TM3 and TM6 as well.

Experimental Probing of the 6.44–7.49 Interaction

The existence and functional role of this predicted TM6-TM7 interaction was probed by mutating the residues involved and testing the functional consequences after transfection of the mutant constructs in COS-7 cell. The following mutants were engineered: (i) the D*6.44*N/N7*.49*D double mutant, made in order to mimic the situation of the *Drosophila* receptor in the context of the human TSHr; (ii) D*6.44*N and N7*.49*D single mutants, introduced in order to explore the effects of the individual mutations; (iii) D*6.44*A and N7*.49*A side chain deletion mutants engineered to test the effects of eliminating altogether

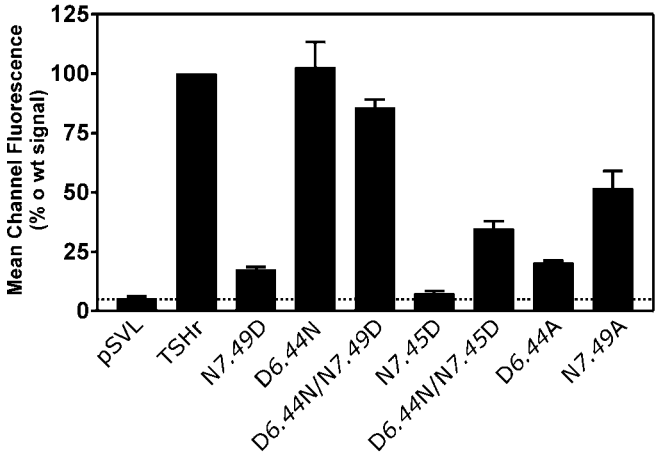

FIG. 3. **Level of expression of the receptors.** Cell surface expression of wt TSHr and the different mutants measured by FACS using the BA8 monoclonal antibody which recognizes a conformational epitope in the NH_2-terminal domain of the receptor. The data are representative of at least four different experiments. Values represent mean cell fluorescence, normalized to the value obtained for wt TSHr (*error bars*: S.E.).

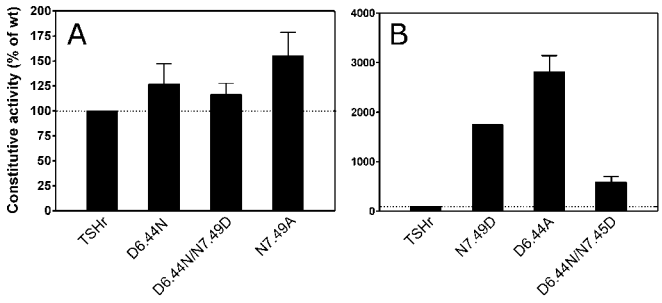

FIG. 4. **Normalized constitutive activity of wt and mutant receptors.** Basal cAMP accumulation was measured for each receptor and normalized to the cell-surface expression (see "Experimental Procedures"). Values are averages of at least three experiments, and were re-scaled as percentages of wt basal activity (*error bars*: S.E.).

the interactions between these side chains and any other residue. Following observations made from our molecular dynamics simulation of the TSHr and other studies on the LH/CG receptor (24) we designed two additional mutants, the single N7.*45*D substitution and the double substitution D*6.44*N/N7.*45*D. This was done in order to explore the possibility of a direct interaction between D*6.44* and N7.*45*.

Cell Surface Expression of the Mutants

Cell surface expression of the mutated receptors was measured by FACS analysis using the BA8 monoclonal antibody (36). As the epitope of the BA8 antibody is located in the NH_2-terminal region of the TSHr (1), we do not expect a modification of its affinity following mutations in the transmembrane region. Also, similar results were obtained with another monoclonal antibody (3G4), recognizing a different epitope in the ectodomain (not shown). Hence, it is assumed that observed fluorescence changes will be in direct relation with the number of receptors present at the cell surface. As shown in Fig. 3, mutants D*6.44*N, D*6.44*N/N7.*49*D, and N7.*49*A are expressed at levels comparable (above 50%) to that of the wild type TSHr. In contrast, mutants N7.*49*D, D*6.44*A, and the D*6.44*N/N7.*45*D double mutant display a reduced expression, between 15 and 30% of the wild type receptor expression. The level of expression of N7.*45*D is too low (specific fluorescence of about 3% of wt TSHr) to allow reliable normalization of functional results, it will therefore not be considered further.

Basal and TSH-stimulated cAMP Accumulation in COS-7 Cells Transfected with the Mutants

The constitutive activity of the wt and mutant receptors was characterized by measuring intracellular cAMP accumulation in transiently transfected COS-7 cells. As constitutive activity is linearly dependent on the number of receptors at the cell surface (39), we have normalized the basal activity of each construct using cell surface expression data yielded by FACS analyses (see "Experimental Procedures"). This allows to compute constitutive activity on a *per receptor* basis, and to compare it to that of the wild type receptor.

Mutants D*6.44*N, D*6.44*N/N7.*49*D, and N7.*49*A display basal activity similar to that of the wild type (Fig. 4*A*). Strikingly, the single mutants N7.*49*D and D*6.44*A show a dramatic increase in constitutive activity, reaching more than 15 times that of wild type TSHr, when normalized to the level of expression (Fig. 4*B*). Although the N7.*49*D mutant, bearing aspartate residues at both positions *6.44* (as in wild type) and *7.49* (introduced by mutation), is among the strongest constitutive mutant of the TSHr ever identified (37), it is remarkable that addition of the D*6.44*N mutation on the N7.*49*D background reverses completely the phenotype back to a wild type-like behavior. The D*6.44*N/N7.*45*D can also be considered as a constitutive mutant as its basal activity is more than five times that of wt TSHr (Fig. 4*B*).

We then tested the ability of TSH to stimulate the various constructs. Fig. 5 illustrates typical concentration-response curves and the corresponding EC_{50} are summarized in Table I.

All mutants except N7.*49*A are stimulated by TSH in a way similar to the wild type. While starting from a higher basal level, the N7.*49*D mutant is activated efficiently by TSH, reaching comparable E_{max} (not shown). All EC_{50} values were in the range 0.4–1 milliunits/ml of TSH (Fig. 5, *A* and *B*, and Table I). Although the N7.*49*A mutant displays wt-like constitutive activity, TSH is unable to elicit signal transduction, as only very moderate stimulation if any can be observed at 100 milliunits/ml, a saturating concentration for wt TSHr (Fig. 5*C*).

Hormone Binding

The binding properties of the different receptors were tested by homologous competition using ^{125}I-bovine TSH as tracer. As shown in Fig. 6, all constructs tested were able to bind TSH efficiently.

Mutants D*6.44*N and D*6.44*N/N7.*49*D bind TSH with similar affinity as the wild type receptor, as measured by the IC_{50} test (IC_{50} of about 3 milliunits/ml, see Table I and Fig. 6*A*). Noticeably, the various constitutive mutants display a significantly lower IC_{50} (below 1 milliunits/ml, see Table I and Fig. 6*B*). Increase in apparent affinity with no significant modification of hormone potency has been observed in most constitutive mutants of the TSH receptor (40). Interestingly, mutant N7.*49*A binds TSH with high affinity, even slightly higher than the wt receptor (Fig. 6*A* and Table I), although this mutant is completely unable to be activated by the hormone.

It should be noted that the residues identified here as key actors in the activation mechanism of the TSHr have also been studied by several groups on the LH receptor (24, 41). Overall these studies are in agreement with the results presented here. Note, however, that these studies did not consider double mutants in different TMs, which in our view are crucial to the identification of TM6-TM7 interactions.

Molecular Dynamics Simulations of the Transmembrane Region of Mutant Receptors

In an effort to interpret, in structural terms, the results of the site-directed mutagenesis experiments, the molecular dy-

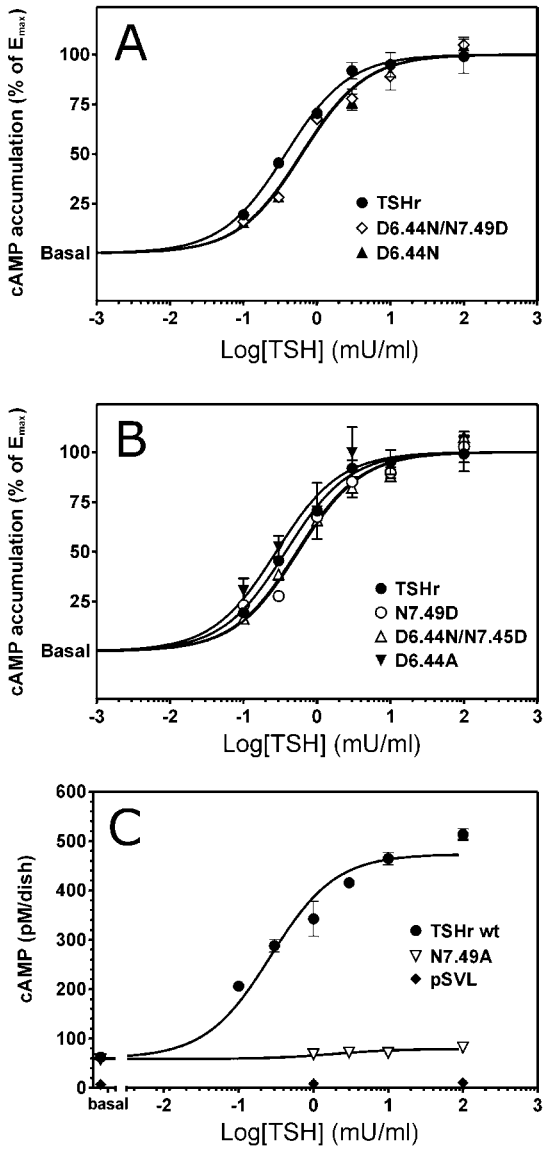

FIG. 5. **TSH stimulation of the different receptors.** TSH-induced cAMP increase in the different cell lines. The *curves* represent a typical experiment out of at least three, performed independently. Results were analyzed by nonlinear regression using the GraphPad Prism software. Data were normalized between basal and maximum values (E_{max}) in *panel A* and *B*. *A,* receptors with (close to) normal basal activity. *B,* receptors with strongly increased basal activity, together with the wt receptor. *C,* wt TSHr and N7.49A mutant. Absolute cAMP values are shown in this panel, demonstrating the inability of TSH to induce significant response in the mutant.

namics trajectories of the transmembrane region of TSHr featuring the different mutants were analyzed, with focus on the region between TM6 and TM7, surrounding the mutated residues. In particular, we monitored all possible interactions between the various polar groups in the vicinity of *6.44* and *7.49*, which were involved in the local hydrogen bond network in the wt TSHr trajectory. Representative structures of the mutant trajectories are shown in Fig. 2.

The D6.44N Mutant Receptor—Notwithstanding the absence of the acid group, the D*6.44*N mutant was found to maintain polar interactions between TM6 and TM7 (see Fig. 2). Residue N*6.44* interacts with N7.*49* through two hydrogen bonds. One forms persistently between the $O_{\delta1}$ atom of N*6.44* and the $N_{\delta2}H$ group of N7.*49* (average O-H distance of 2.0 Å). The other forms in 40% of the conformations, between the $N_{\delta2}H$ group of N*6.44* and the $O_{\delta1}$ atom of N7.*49* (average O-H distance of *2.2* Å). The same $N_{\delta2}H$ group also H bonds to the backbone oxygen in the preceding turn of the TM6 helix. We find moreover that the TM6-TM7 link is reinforced by an additional H-bond, between the $O_{\gamma1}H$ of T*6.43* and the $O_{\delta1}$ of N7.*49* (average O-H distance, 1.8 Å).

The D6.44N/N7.49D Double Mutant Receptor—The representative structure for the trajectory of this mutant receptor TM region features a hydrogen bond network opposite to that seen in the wild type simulation (see Fig. 2). The negatively charged D7.*49* interacts with the neutral N*6.44*, through a $N_{\delta2}^{6.44}H\text{-}O_{\delta1}^{7.49}$ hydrogen bond (average distance, 1.8 Å). In addition, its $O_{\delta1}$ and $O_{\delta2}$ atoms take turns in forming an H-bond with the $N_{\delta1}H$ group of N7.*45* (average minimum distance of 1.9 Å). Furthermore the $O_{\delta1}$ of N*6.44* forms hydrogen bonds to both the $N_{\delta2}H$ of N7.*45* (2.2 Å), and the $O_{\delta}H$ of S*3.39* (1.9 Å), mimicking the hydrogen bond network seen in the wt simulations.

The N7.49D Mutant Receptor—The molecular dynamics simulation of the constitutive N7.*49*D mutant receptor shows a dramatic change in the hydrogen bond network linking TM6 and TM7 (see Fig. 2). Due to the repulsion between the *6.44* and *7.49* side chains, both an aspartate in this mutant, the D*6.44* side chain has moved away from TM7 and toward TM3, forming two new persistent H-bonds. One with S*3.36* ($O_{\delta}^{3.36}H\text{-}O_{\delta1}^{6.44}$, average distance 1.7 Å), and one with S*3.39* ($O_{\delta}^{3.39}H\text{-}O_{\delta2}^{6.44}$, average distance 2.1 Å). On the other hand, D7.*49* forms H-bonds with the $N_{\delta2}H$ of N7.*45* (average distance 1.8 Å) and with the $O_{\gamma1}H$ of T*6.43* (average distance 2.2 Å), via its $O_{\delta1}$ and $O_{\delta2}$ atoms, respectively.

The D6.44N/N7.45D Double Mutant Receptor—In this mutant receptor polar interactions between helices TM6 and TM7 are maintained throughout the trajectory, but their pattern differs from that observed in the wt. They are formed between residues N*6.44* and T*6.43* on the one hand, and D7.*45* and N7.*49* on the other. An H-bond forms persistently between the N*6.44* $N_{\delta2}H$ and the D7.*45* $O_{\delta1}$ (average distance, 1.9 Å). N*6.44* also H-bonds to N7.*49* in a sizable fraction of the conformations, but not as persistently as in the wt simulations. In addition, the D7.*45* $O_{\delta1}$ hydrogen bonds persistently to the T*6.43* $O_{\gamma1}H$ (average distance, 1.7 Å). To form this pattern of interactions, TM6 and TM7 have undergone a small local rearrangement, which now enables H-bond formation between the N7.*49* $N_{\delta2}H$ and D*2.50* $O_{\delta1}$ (average distance 2.5 Å). The latter residue is the highly conserved Asp in TM2, found in most rhodopsin-like GPCRs (see "Discussion").

The D6.44A Mutant Receptor—In the absence of a polar side chain at *6.44*, the interactions of TM6 with N7.*45* and N7.*49* in TM7 can no longer be made. As a consequence, the latter polar side chains rearrange their respective conformations, so as to find new H-bonding partners. N7.*49* rotates toward TM2, forming an H-bond between its $N_{\delta2}H$ group and the D*2.50* $O_{\delta2}$ (average distance 2.0 Å) (Fig. 2). This interaction too is facilitated by a local rearrangement of TM7 which brings *7.49* closer to *2.50* than in the wt simulation (data not shown).

The N7.49A Mutant Receptor—Unlike for the *D6.44A* mutant, in this mutant, polar interactions between TM6 and TM7 are maintained through H-bonds of D*6.44* to N7.*45* ($N_{\delta2}^{7.45}H\text{-}O_{\delta2}^{6.44}$, average distance, 1.8 Å) and to T*6.43* ($O_{\gamma1}^{6.43}H\text{-}O_{\delta1}^{6.44}$, average distance, 1.9 Å) (see Fig. 2).

In summary, the nonconstitutive mutant receptors (D*6.44*N, D*6.44*N/N*7.49*D, and N*7.49*A*)* maintain the TM6-TM7 interaction through a complex hydrogen bond network involving the side chains at positions *3.39*, *6.43*, *6.44*, *7.45*, and *7.49*. Moreover, as in the wt simulation, the side chain of residue *7.49* is always maintained close to TM6 (except in the N7.*49*A mutant), essentially through direct partnership with residue *6.44*.

TABLE I

Binding and functional properties of wt TSHr and mutant receptors

Binding and functional parameters were measured on COS 7-transfected cells as described under "Experimental Procedures." EC_{50} and IC_{50} are expressed in milliunits/ml of TSH. Values represent the mean ± S.E. of at least three independent determinations. No EC_{50} could be obtained for the N7.*49*A mutant as this mutant was not stimulated by TSH.

	EC_{50}		IC_{50}	
	Average	S.E.	Average	S.E.
Wt	0.60	*0.09*	3.06	*0.28*
N7.*49*D	0.65	*0.02*	0.89	*0.13*
D*6.44*N	0.78	*0.17*	3.44	*0.49*
D*6.44*N/N7.*49*D	0.77	*0.13*	3.08	*0.47*
N7.*45*D	0.38	*0.19*	0.92	*0.31*
D*6.44*A	0.94	*0.28*	0.88	*0.15*
D*6.44*N/N7.*45*D	0.67	*0.20*	2.10	*0.35*
N7.*49*A			1.70	*0.05*

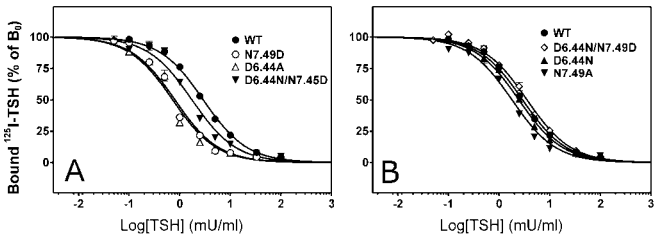

FIG. 6. **Binding properties of the wt and mutant receptors.** Homologous competition binding assays on COS-7 cell lines expressing the wt TSHr and the different mutants, using ^{125}I-TSH as tracer. The data are representative of at least three experiments. Results were analyzed by the GraphPad Prism software, using a single site model, and the data were normalized for nonspecific (0%) and specific binding in the absence of competitor (100%). All points were run in duplicate (*error bars*: S.E.).

The least active of the constitutive mutant receptors (D*6.44*N/N7.*45*D) maintains the TM6-TM7 link but there is a clear re-orientation of the N7.*49* side chain toward D*2.50*. The most constitutive mutant receptors (N7.*49*D and D*6.44*A) do not maintain the TM6-TM7 interaction, and especially the orientation of residue *7.49*, which moves away from TM6.

DISCUSSION

A 6.44–7.49 Link Maintains the Inactive State of the TSHr—On the basis of multiple alignment of glycohormone receptors, we have identified in the sequence of a putative *Drosophila* receptor (6) an exchange between two highly conserved residues: Asp*6.44* and Asn*7.49*. These two residues are spatially close to each other in the rhodopsin template, suggesting a possible direct interaction. In addition, the observation that a variety of spontaneous mutations affecting D*6.44* in both the TSHr and LHr increase their constitutive activity, pointed to a possible role of D*6.44* (and thus of the postulated *6.44–7.49* interaction) in the activation mechanism.

In this context, mutation of N7.*49* to Asp is expected to abrogate this putative interaction between residues *6.44* and *7.49*, owing to electrostatic repulsion between the 2 negatively charged side chain, which should be rescued by the complementary mutation of D*6.44* to Asn. The functional characteristics of these mutants fulfill nicely these expectations when assayed in COS cells: the N7.*49*D mutant displays a very strong increase in basal activity, reaching more than 15 times that of the wild type receptor, whereas the D*6.44*N/N*6.49*D double mutant behaves as the wild type receptor. Together with the reciprocal amino acid exchange observed at these positions in the *Drosophila* receptor the simplest explanation is that these two residues are close in space and do interact with each other. Similar reasoning and experimental approaches have been used in the study of other receptors (42–44). Interestingly, they supported the idea that the same N7.*49* residue would interact with D*2.50*, one of the most conserved residues in rhodopsin-like GPCRs. The apparent incompatibility between these two mutually exclusive interactions find an explanation in the study of additional mutants (see below).

Our molecular dynamics study of the helix bundle of the TSHr based on the crystal structure of rhodopsin strongly supports the D*6.44*-N7.*49* interaction. In simulations of the wild type TSHr structure, the D*6.44*-N7.*49* interaction was observed in all conformations of the trajectory, indicating that this putative partnership fits well the rhodopsin template, under our simulation conditions. In agreement with experimental observations, simulation of the D*6.44*N/N7.*49*D double mutant shows that the interaction between these amino acids is preserved when the two side chains are exchanged, as found in the *Drosophila* receptor. It should be noted that our modeling study predicts that a *6.44-7.49* interaction would be preserved in the D*6.44*N single mutant, and, indeed, when tested experimentally, this mutant showed a wild type-like behavior. This observation is of particular significance, considering that most if not all other mutations at this position induce constitutive activity in the TSH or LH receptors (35, 41). The structural rationale explaining why only Asn is tolerated at position *6.44* in the glycohormone receptors gives support to the local structure proposed here and suggests an explanation as to how the D*6.44*N/N*6.49*D double substitution may have occurred stepwise in evolution in the *Drosophila* receptor.

Our modeling points to additional partners to account for the phenotype of some of the constitutive mutants identified here. The strongest constitutive activity is associated with a complete lack of the *6.44-7.49* interaction (like the N7.*49*D and D*6.44*A mutants). Weakening of this bond as observed in the D*6.44*N/N7.*45*D double mutant causes increase in constitutive activity but to a smaller extent, which indicates that this mutant is not completely released from its ground state constraints. In our N7.*49*D simulation, D*6.44* interacts with serine residues S*3.36*^{505} and S*3.39*^{508}, in TM3. Interestingly mutations of S*3.36* into Arg or Asn were found to constitutively activate the receptor (40, 45). It is likely that the *3.36-6.44* interaction observed in the N7.*49*D mutant would be strongly favored in a S*3.36*^{505}R mutant. An ionic R*3.36*-D*6.44* interaction would be more stable than the D*6.44*-N7.*49* (wt situation), therefore redirecting the side chain of D*6.44* toward TM3 and releasing N7.*49*.

Sequestration of N7.49 Is Implicated in the Inactive Conformation of the TSHr—Overall the modeling and experimental data converge toward the idea that, in the TSHr, a direct D*6.44*-N7.*49* interaction is required to maintain the inactive state of the receptor, and that breaking this link results in high constitutive activity. How does this view agree with current notions of activation of other rhodopsin-like GPCRs?

Despite the fact that residue D*6.44* is not conserved throughout the family (in most cases it is a Phe), mutation of *6.44* into Ala leads also to constitutive activation in other rhodopsin-like receptors (46, 47). Moreover, in the opsins, *6.44* has been shown to be linked to the activation process, being involved in color sensitivity (48, 49). The mechanism by which Asp (in the glycohormone receptors) or Phe (in most of the others) might exert similar functions cannot be determined from the present study. A provocative explanation could be that sequestration of the side chain of N7.*49* by H-bonding to D*6.44* in the inactive TSHr would be replaced by the existence of a steric shield in the other GPCRs.

An Active Role of N7.49 in Signal Transduction—Mutation of N7.*49* into Ala casts another light on the role of the TM6-TM7

motif in the activation of the TSHr. Although the N7.*49*A mutant binds TSH with wild type-like affinity, it is totally refractory to activation by the hormone. This indicates that disrupting the *6.44-7.49* interaction (which is *de facto* absent here) is not sufficient to trigger activation, but that N7.*49* is fulfilling a specific role during activation, which cannot be achieved by an Ala side chain. Work on various rhodopsin-like GPCRs have suggested that, upon activation, N7.*49* would interact with the highly conserved Asp of TM2 (D*2.50*) and also with the perfectly conserved Asn of TM1 (N*1.50*) (42, 43). As already mentioned, using a similar experimental strategy as the one described here, it has been shown in these studies that inactivation by a D*2.50*N mutation could be rescued by an additional N7.*49*D mutation. Moreover, it has been proposed that D*2.50* undergoes a change in H-bonding upon light activation of rhodopsin (50).

A Model of the Early Steps of Activation—We can summarize the different points discussed above in a simple sequence of intramolecular events that would be necessary to trigger the conformational changes leading to activation.

(i) In the inactive state of the receptor, N7.*49* is locked away from TM2. In the glycohormone receptor family, this conformational constraint is achieved by a direct interaction with D*6.44*.

(ii) A necessary step in activation would be the release of this interaction. This could happen either upon ligand binding, or due to mutation of a key residue. For instance, the D*6.44*A mutation abrogates completely the interaction. Noticeably, this mutation leads to almost maximal activation (2/3 of activity after full stimulation by the hormone).

(iii) N7.*49* would then reorient toward the *1.50-2.50* motif, where it could modify the polar equilibrium and subsequently cause a reorganization of the inter-helical H-bond network. This rearrangement would in turn induce the conformational changes of the TM bundle known to be associated with activation (*i.e.* motions of TM3 and TM6 (51, 52)). In the N7.*49*A mutant, the side chain of A7.*49* would not be able to establish the interaction(s) normally fostered by the Asn, and no transition to the active state is observed. Whether this scenario applies to the physiological activation of the receptor by its natural agonist remains to be demonstrated.

The *2.50-7.49* interaction is well supported by numerous studies on various receptors. However, a survey of the GPCR data base yields about 100 sequences of rhodopsin-like receptors with an Asp residue at both the *2.50* and *7.49* positions. In this case a direct *2.50-7.49* interaction is impossible. It has been shown that an Asn to Asp substitution at position *7.49* leads to modification of the signaling characteristics in GPCRs: changing the N7.*49*P*XX*Y motif for D7.*49*P*XX*Y leads to changes in the coupling specificity of the GnRH receptor (53). This indicates that the active conformation achieved by receptors bearing an Asp in *7.49* may be somewhat different from that of those bearing an Asn, in agreement with the current concept that GPCRs may achieve multiple active states with the potential to activate different G proteins (52).

When integrated with the current literature, the present results point to the *1.50-2.50-7.49* motif as an important actor in the activation of rhodopsin-like GPCRs. Additional players are likely to be involved as well, which remain to be identified. Among these are positively charged residue(s), participation of structural water molecules and specific protonations. In this context, it was suggested that D*2.50* would interact with the conserved R*3.50* of the DRY motif at the base of TM3 (54, 55). However, since the C_α of these two residues are separated by more than 24 Å in the crystal structure of rhodopsin, we do not currently favor such a possibility. Positively charged residues are often found at the cytoplasmic end of TM6 and could possibly interact with the *1.50-2.50-7.49* motif after a rigid body motion of TM6 of the kind which is believed to occur upon activation (56–58). It is noteworthy that a water molecule is present in close vicinity of D*2.50* in one of the two monomers of the rhodopsin crystal structure (22). Also, it is known that protonation events do take place upon activation of GPCRs. One of the protonation site is most probably the highly conserved D*3.49* of the DRY motif (59). Recent studies on the β_2-adrenergic receptor indicate that protonation of an additional negatively charged residue is most probably implicated in activation (60). D*2.50* is a good candidate for the "missing" protonated residue in adrenergic receptors and has been proposed to be protonated in rhodopsin (50, 61). Protonation of D*2.50* could be a necessary step in the activation process, as it has been shown for several receptors that a D*2.50*N mutation severely impairs the signaling properties, while a D*2.50*E mutation can be tolerated (44). Protonation of D*2.50* would account for the observation that the N*1.50*-D*2.50*-N7.*49* motif tolerates N7.*49*D substitutions in many systems, including the TSH receptor. As we were not able to include the various putative additional players in the molecular dynamics simulations, we could not observe a *2.50-7.49* interaction in our model of the N7.*49*D mutant. In all fairness, the absence of these players in our simulations and for that matter, also that of the entire extracellular domain and of an explicit lipid environment, are limitations that must be kept in mind also when considering other conclusions deduced from the simulations.

The Active Conformation of the Wild Type Receptor May Be Different from that of D6.44 Mutants—Of potential interest is the observation that the N7.*49*A mutant, while it cannot be activated by the hormone, still displays constitutive activity similar to the wild type TSHr. This implies that the interactions achieved by the side chain of N7.*49* would be dispensable for the basal activity of the wild type receptor, whereas they are required for that of the ligand induced activity. The existence of multiple active conformations of GPCRs has been well documented in the case of TSHr mutants (16, 62) as well as in many other GPCRs (see Ref. 52 for review). The present observation suggests that "noisy" receptors like the unliganded wild type TSHr might achieve an active conformation via a route involving residues distinct from those implicated in full agonist-induced activation.

In conclusion, we have identified a conserved motif central to the activation of the TSH receptor. Our molecular modeling provides a structural framework for understanding how the D*6.44*-N7.*49* link, by sequestrating the side chain of N7.*49*, would keep it in an "inactive" conformation. Upon activation, this side chain would be released, and free to adopt its "active" conformation, which involves interactions with the N*1.50*-D*2.50* motif. Further rearrangements of the intramolecular network, which remain to be defined, lead to exposure of surfaces allowing interaction between the receptor and its cognate G protein(s). We suggest that in other GPCRs, a similar mechanism might operate, but involving a different type of partner for N7.*49* in the inactive state. Now that rhodopsin provides a reliable template for modeling the inactive conformation of GPCRs, it is our hope that further molecular dynamics simulations coupled to site-directed mutagenesis experiments will help in elucidating their active conformation(s).

Acknowledgments—We thank Claude Massart for expert technical assistance and Jean Richelle for valuable help with the computer systems. We are grateful to BRAHMS Diagnostica (Berlin, Germany) for providing radiolabeled bovine TSH. We thank the Center de Computació i Comunicacions de Catalunya for use of the computer facilities.

REFERENCES

1. Costagliola, S., Khoo, D., and Vassart, G. (1998) *FEBS Lett.* **436,** 427–433
2. Da Costa, C. R., and Johnstone, A. P. (1998) *J. Biol. Chem.* **273,** 11874–11880

3. Kajava, A. V., Vassart, G., and Wodak, S. J. (1995) *Structure* **3,** 867–877
4. Kobe, B., and Deisenhofer, J. (1995) *Curr. Opin. Struct. Biol.* **5,** 409–416
5. Kajava, A. V. (1998) *J. Mol. Biol.* **277,** 519–527
6. Hauser, F., Nothacker, H. P., and Grimmelikhuijzen, C. J. (1997) *J. Biol. Chem.* **272,** 1002–1010
7. Nothacker, H. P., and Grimmelikhuijzen, C. J. (1993) *Biochem. Biophys. Res. Commun.* **197,** 1062–1069
8. Eriksen, K. K., Hauser, F., Schiott, M., Pedersen, K. M., Sondergaard, L., and Grimmelikhuijzen, C. J. (2000) *Genome Res.* **10,** 924–938
9. Wilson, R., Ainscough, R., Anderson, K., Baynes, C., Berks, M., Bonfield, J., Burton, J., Connell, M., Copsey, T., and Cooper, J. (1994) *Nature* **368,** 32–38
10. Hsu, S. Y., Liang, S. G., and Hsueh, A. J. (1998) *Mol. Endocrinol.* **12,** 1830–1845
11. Hsu, S. Y., Kudo, M., Chen, T., Nakabayashi, K., Bhalla, A., van der Spek, P. J., van Duin, M., and Hsueh, A. J. (2000) *Mol. Endocrinol.* **14,** 1257–1271
12. Parma, J., Duprez, L., Van Sande, J., Cochaux, P., Gervy, C., Mockel, J., Dumont, J., and Vassart, G. (1993) *Nature* **365,** 649–651
13. Duprez, L., Parma, J., Van Sande, J., Allgeier, A., Leclere, J., Schvartz, C., Delisle, M. J., Decoulx, M., Orgiazzi, J., Dumont, J., and Vassart, G. (1994) *Nat. Genet.* **7,** 396–401
14. Kosugi, S., Okajima, F., Ban, T., Hidaka, A., Shenker, A., and Kohn, L. D. (1992) *J. Biol. Chem.* **267,** 24153–24156
15. Refetoff, S., Dumont, J. E., and Vassart, G. (2001) in *The Metabolic & Molecular Basis of Inherited Disease* (Scriver, C. R., Beaudet, A. L., Sly, W. S., and Valle, D., eds) pp. 4029–4076, McGraw-Hill, New York
16. Biebermann, H., Schoneberg, T., Schulz, A., Krause, G., Gruters, A., Schultz, G., and Gudermann, T. (1998) *FASEB J.* **12,** 1461–1471
17. Sunthornthepvarakui, T., Gottschalk, M. E., Hayashi, Y., and Refetoff, S. (1995) *N. Engl. J. Med.* **19,** 332; 155–160
18. de Roux, N., Misrahi, M., Brauner, R., Houang, M., Carel, J. C., Granier, M., Le Bouc, Y., Ghinea, N., Boumedienne, A., Toublanc, J. E., and Milgrom, E. (1996) *J. Clin. Endocrinol. Metab.* **81,** 4229–4235
19. Themmen, A. P. N., and Huhtaniemi, I. T. (2000) *Endocr. Rev.* **21,** 551–583
20. Kudo, M., Osuga, Y., Kobilka, B. K., and Hsueh, A. J. (1996) *J. Biol. Chem.* **271,** 22470–22478
21. Gromoll, J., Simoni, M., and Nieschlag, E. (1996) *J. Clin. Endocrinol. Metab.* **81,** 1367–1370
22. Palczewski, K., Kumasaka, T., Hori, T., Behnke, C. A., Motoshima, H., Fox, B. A., Le, T. I., Teller, D. C., Okada, T., Stenkamp, R. E., Yamamoto, M., and Miyano, M. (2000) *Science* **289,** 739–745
23. Shenker, A., Laue, L., Kosugi, S., Merendino, J. J., Jr., Minegishi, T., and Cutler, G. B., Jr. (1993) *Nature* **365,** 652–654
24. Angelova, K., Narayan, P., Simon, J. P., and Puett, D. (2000) *Mol. Endocrinol.* **14,** 459–471
25. Lin, Z., Shenker, A., and Pearlstein, R. (1997) *Protein Eng.* **10,** 501–510
26. Chelvanayagam, G., Eggenschwiler, A., Knecht, L., Gonnet, G. H., and Benner, S. A. (1997) *Protein Eng.* **10,** 307–316
27. Larson, S. M., Di Nardo, A. A., and Davidson, A. R. (2000) *J. Mol. Biol.* **303,** 433–446
28. Ballesteros, J. A., and Weinstein, H. (1995) *Methods Neurosci.* **25,** 366–428
29. McGregor, M. J., Islam, S. A., and Sternberg, M. J. (1987) *J. Mol. Biol.* **20,** 198; 295–310
30. Aqvist, J., and Luzhkov, V. (2000) *Nature* **20,** 404, 881–884
31. Darden, T., York, D., and Pedersen, L. (1993) *J. Chem. Phys.* **98,** 10089–10092
32. Case, D. A., Pearlman, D. A., Caldwell, J. W., Cheatham, T. E., Ross, W. S., Simmerling, C. L., Darden, T. A., Merz, K. M., Stanton, R. V., Cheng, A. L., Vincent, J., Crowley, M., Ferguson, D. M., Radmer, R. J., Seibel, G. L., Singh, U. C., Weiner, P. K., and Kollman, P. A. (1997) *AMBER5*, University of California, San Francisco
33. Cornell, W. D., Cieplak, P., Bayly, C. I., Gould, I. R., Merz, K. M., Jr., Ferguson, D. M., Spellmeyer, D. C., Fox, T., Caldwell, J. W., and Kollman, P. A. (1995) *J. Am. Chem. Soc.* **117,** 5179–5197
34. Libert, F., Lefort, A., Gerard, C., Parmentier, M., Perret, J., Ludgate, M., Dumont, J. E., and Vassart, G. (1989) *Biochem. Biophys. Res. Commun.* **165,** 1250–1255
35. Parma, J., Duprez, L., Van Sande, J., Hermans, J., Rocmans, P., Van Vliet, G., Costagliola, S., Rodien, P., Dumont, J. E., and Vassart, G. (1997) *J. Clin. Endocrinol. Metab.* **82,** 2695–2701
36. Costagliola, S., Rodien, P., Many, M. C., Ludgate, M., and Vassart, G. (1998) *J. Immunol.* **160,** 1458–1465
37. Van Sande, J., Parma, J., Tonacchera, M., Swillens, S., Dumont, J., and Vassart, G. (1995) *J. Clin. Endocrinol. Metab.* **80,** 2577–2585
38. Horn, F., Weare, J., Beukers, M. W., Horsch, S., Bairoch, A., Chen, W., Edvardsen, O., Campagne, F., and Vriend, G. (1998) *Nucleic Acids Res.* **26,** 275–279
39. Van Sande, J., Swillens, S., Gerard, C., Allgeier, A., Massart, C., Vassart, G., and Dumont, J. E. (1995) *Eur. J. Biochem.* **229,** 338–343
40. Tonacchera, M., Van Sande, J., Cetani, F., Swillens, S., Schvartz, C., Winiszewski, P., Portmann, L., Dumont, J. E., Vassart, G., and Parma, J. (1996) *J. Clin. Endocrinol. Metab.* **81,** 547–554
41. Kosugi, S., Mori, T., and Shenker, A. (1996) *J. Biol. Chem.* **271,** 31813–31817
42. Sealfon, S. C., Chi, L., Ebersole, B. J., Rodic, V., Zhang, D., Ballesteros, J. A., and Weinstein, H. (1995) *J. Biol. Chem.* **270,** 16683–16688
43. Perlman, J. H., Colson, A. O., Wang, W., Bence, K., Osman, R., and Gershengorn, M. C. (1997) *J. Biol. Chem.* **272,** 11937–11942
44. Donnelly, D., Maudsley, S., Gent, J. P., Moser, R. N., Hurrell, C. R., and Findlay, J. B. (1999) *Biochem. J.* **339,** 55–61
45. Fuhrer, D., Holzapfel, H. P., Wonerow, P., Scherbaum, W. A., and Paschke, R. (1997) *J. Clin. Endocrinol. Metab* **82,** 3885–3891
46. Baranski, T. J., Herzmark, P., Lichtarge, O., Gerber, B. O., Trueheart, J., Meng, E. C., Iiri, T., Sheikh, S. P., and Bourne, H. R. (1999) *J. Biol. Chem.* **274,** 15757–15765
47. Spalding, T. A., Burstein, E. S., Henderson, S. C., Ducote, K. R., and Brann, M. R. (1998) *J. Biol. Chem.* **273,** 21563–21568
48. Chan, T., Lee, M., and Sakmar, T. P. (1992) *J. Biol. Chem.* **267,** 9478–9480
49. Asenjo, A. B., Rim, J., and Oprian, D. D. (1994) *Neuron* **12,** 1131–1138
50. Rath, P., DeCaluwe, L. L., Bovee-Geurts, P. H., DeGrip, W. J., and Rothschild, K. J. (1993) *Biochemistry* **32,** 10277–10282
51. Wess, J., Nanavati, S., Vogel, Z., and Maggio, R. (1993) *EMBO J.* **12,** 331–338
52. Gether, U. (2000) *Endocr. Rev.* **21,** 90–113
53. Mitchell, R., McCulloch, D., Lutz, E., Johnson, M., MacKenzie, C., Fennell, M., Fink, G., Zhou, W., and Sealfon, S. C. (1998) *Nature* **392,** 411–414
54. Ballesteros, J., Kitanovic, S., Guarnieri, F., Davies, P., Fromme, B. J., Konvicka, K., Chi, L., Millar, R. P., Davidson, J. S., Weinstein, H., and Sealfon, S. C. (1998) *J. Biol. Chem.* **273,** 10445–10453
55. Scheer, A., Fanelli, F., Costa, T., De Benedetti, P. G., and Cotecchia, S. (1997) *Proc. Natl. Acad. Sci. U. S. A.* **94,** 808–813
56. Javitch, J. A., Fu, D., Liapakis, G., and Chen, J. (1997) *J. Biol. Chem.* **272,** 18546–18549
57. Gether, U., Lin, S., Ghanouni, P., Ballesteros, J. A., Weinstein, H., and Kobilka, B. K. (1997) *EMBO J.* **16,** 6737–6747
58. Farrens, D. L., Altenbach, C., Yang, K., Hubbell, W. L., and Khorana, H. G. (1996) *Science* **274,** 768–770
59. Fahmy, K., Sakmar, T. P., and Siebert, F. (2000) *Biochemistry* **39,** 10607–10612
60. Ghanouni, P., Schambye, H., Seifert, R., Lee, T. W., Rasmussen, S. G., Gether, U., and Kobilka, B. K. (2000) *J. Biol. Chem.* **275,** 3121–3127
61. Fahmy, K., Jager, F., Beck, M., Zvyaga, T. A., Sakmar, T. P., and Siebert, F. (1993) *Proc. Natl. Acad. Sci. U. S. A.* **90,** 10206–10210
62. Parma, J., Van Sande, J., Swillens, S., Tonacchera, M., Dumont, J., and Vassart, G. (1995) *Mol. Endocrinol.* **9,** 725–733